Available online at www.eccomasproceedia.org
Eccomas Proceedia COMPDYN (2025) 462 -46 2

ECCOMAS
Proceedia

COMPDYN 2025
10th ECCOMAS Thematic Conference on
Computational Methods in Structural Dynamics and Earthquake Engineering
M. Papadrakakis, M. Fragiadakis (eds.)
Rhodes Island, Greece, 15-18 June 2025

KINEMATIC RESPONSE OF END-BEARING PILES IN GENERALISED INHOMOGENEOUS SOILS UNDER P-WAVE EXCITATION

Armando Della Corte[1], Stijn François[2], Aggelos Tsikas[3], Jens Vankeirsbilck[4], Jeroen Boydens[4], and George Anoyatis[1]

[1]KU Leuven, Department of Civil Engineering, Hydraulics and Geotechnics Section - Bruges
Spoorwegstraat 12, Bruges, 8200, Belgium
armando.dellacorte@kuleuven.be, george.anoyatis@kuleuven.be

[2] KU Leuven, Department of Civil Engineering, Structural Mechanics Section
Kasteelpark Arenberg 40, Leuven, 3001, Belgium
stijn.francois@kuleuven.be

[3] Quantum Neural Technologies S.A. (QNT)
Patriarchou Ioakeim 34, Athens, 10675, Greece
ait@monogramgroup.eu

[4] KU Leuven, Department of Computer Science, Distributed and Secure Software (DistriNet)
Spoorwegstraat 12, Bruges, 8200, Belgium
jens.vankeirsbilck@kuleuven.be, jeroen.boydens@kuleuven.be

Abstract. *This paper presents a novel elastodynamic model for the analysis of end-bearing piles embedded in generalised continuously inhomogeneous soils, resting on a rigid base and subjected to vertically propagating P-waves. This approach models the pile as a rod, using the strength-of-materials solution, and the soil as an approximate continuum of the Tajimi type. The approximation resides in reducing the number of the elastodynamic equations which govern the soil motion to one, which satisfies the equilibrium in the vertical direction, by eliminating certain stresses and displacements in the soil. The proposed generalised formulation can treat any continuous distribution of the soil stiffness with depth. Soil inhomogeneity is introduced via a generalised power law variation of the soil shear modulus with depth. The response of the pile-soil system is expressed in the form of a generalised Fourier series and the eigenfunctions along the vertical coordinate are captured by employing simple trigonometric functions. The predictive power of the model is verified through comparisons with finite element analyses. Results are presented in terms of kinematic response factors across a wide range of excitation frequencies, soil-pile stiffness contrasts, and types of soil inhomogeneity. It is shown that soil inhomogeneity can reduce the kinematic response factor.*

Keywords: Kinematic Response Factor, Generalised Soil Inhomogeneity, Elastodynamic Model.

ISSN:2623-3347 © 2025 The Authors. Published by Eccomas Proceedia.
Peer-review under responsibility of the organizing committee of COMPDYN 2025.
doi: 10.7712/120125.12762.25695

1 INTRODUCTION

During an earthquake, the seismic excitation experienced at the base of a pile-supported structure may differ substantially from the free surface motions. This complex dynamic phenomenon, observed even in the absence of a superstructure, is commonly termed in the literature kinematic interaction. Several research studies have emphasized the importance of considering kinematic interaction in the seismic design of foundations [1, 2, 3, 4]. Notable seismic events, including Loma Prieta (1989), Northridge (1994), Kobe (1995), and ChiChi (1999), have highlighted the potentially destructive impact of the vertical component of earthquake excitation [5]. These observations suggest that P-waves may dominate seismic design considerations, particularly in cases involving near-fault earthquakes or locations with shallow, rigid rock formations [6]. In this context, the development of rational and cost-effective design tools is essential to assess the effective motion impacting pile-supported structures accurately.

1.1 Available analytical solutions and proposed model

Studies by Mamoon and Ahmad [7] and by Ji and Pak [8] have investigated the seismic response of piles under various wave excitations. Mylonakis and Gazetas [9] introduced a Winkler-type model to capture the kinematic response of piles subjected to vertically propagating P-waves. Subsequent studies introduced more advanced elastodynamic solutions, with Anoyatis et al. [10], Dai et al. [11, 12, 13], and Zheng et al. [14, 15]. Lately, Lin et al. [16] studied the kinematic response of floating piles in two-layered soils excited by P-wave. The studies mentioned earlier are typically limited to scenarios involving either a uniform distribution of soil stiffness with depth or layered soil profiles. More recently, Anoyatis et al. [6] introduced a Tajimi-type solution for the kinematic response of end-bearing piles embedded in a continuously inhomogeneous soil layer. However, this solution applies only to soils where the shear modulus varies linearly with depth. Therefore, the main objective of this study is to provide a novel elastodynamic benchmark solution for the axial kinematic response of end-bearing piles embedded in a generalised continuously inhomogeneous soil deposit. The proposed solution models the pile as a rod and the soil as an approximate continuum of the 'Tajimi' type [17], following the seminal work of Nogami and Novak [18], and the advancements by Anoyatis et al. [19, 20, 21]. The response of both the soil and the pile is expressed in terms of generalised Fourier series of soil modes along the vertical coordinate. These soil modes are captured using a generalised Fourier series and appropriate trigonometric functions to address generalised vertical soil inhomogeneity [22, 23, 24]. In addition to its intrinsic theoretical interest, the proposed model offers advantages over both simpler and more advanced analytical models by effectively addressing any continuous variation of the shear modulus in the vertical direction. Furthermore, it significantly reduces computational complexity compared to more rigorous solutions while maintaining high accuracy. Moreover, the proposed model can serve as a scoping tool in the early design stage and complement numerical analyses by providing a 'benchmark' solution to verify more complex dynamic models. The model's predictive power is assessed through comparisons with finite element analyses in terms of kinematic response factors across various excitation frequencies and soil-pile stiffness ratios.

2 PROBLEM CONSIDERED

The problem examined in this study is depicted in Figure 1. It consists of a single solid vertical pile of length L and circular cross-section of diameter d, embedded in a generalised inhomogeneous soil layer that rests on a rigid rock. The pile is modelled as an elastic rod of Young's modulus E_p and mass density ρ_p according to the strength-of-materials solution. Perfect bonding at the soil-pile interface is assumed. The soil layer is modelled as an approximate continuum of the Tajimi type. It is characterised by its soil mass density ρ_s, Poisson's ratio ν_s, and hysteretic type material damping β_s. Soil inhomogeneity is introduced through a depth-dependent shear modulus defined by the following power-law function:

$$G_\mathrm{s}(z) = G_\mathrm{sH}\left[b + (1-b)\left(\frac{z}{H}\right)\right]^n \tag{1}$$

In Equation (1), z denotes the vertical coordinate, while n and b are dimensionless parameters that define soil inhomogeneity. Specifically, b relates the stiffness at the surface of the layer, G_s0, to the stiffness at its base, G_sH, through the expression $b = (G_\mathrm{s0}/G_\mathrm{sH})^{1/n}$. In the model, hysteretic-type material damping is incorporated through a complex-valued, depth-dependent shear modulus, $G^*_\mathrm{s}(z) = G_\mathrm{s}(z)(1+2i\beta_\mathrm{s})$, where $G_\mathrm{s}(z)$ is defined by Equation (1).

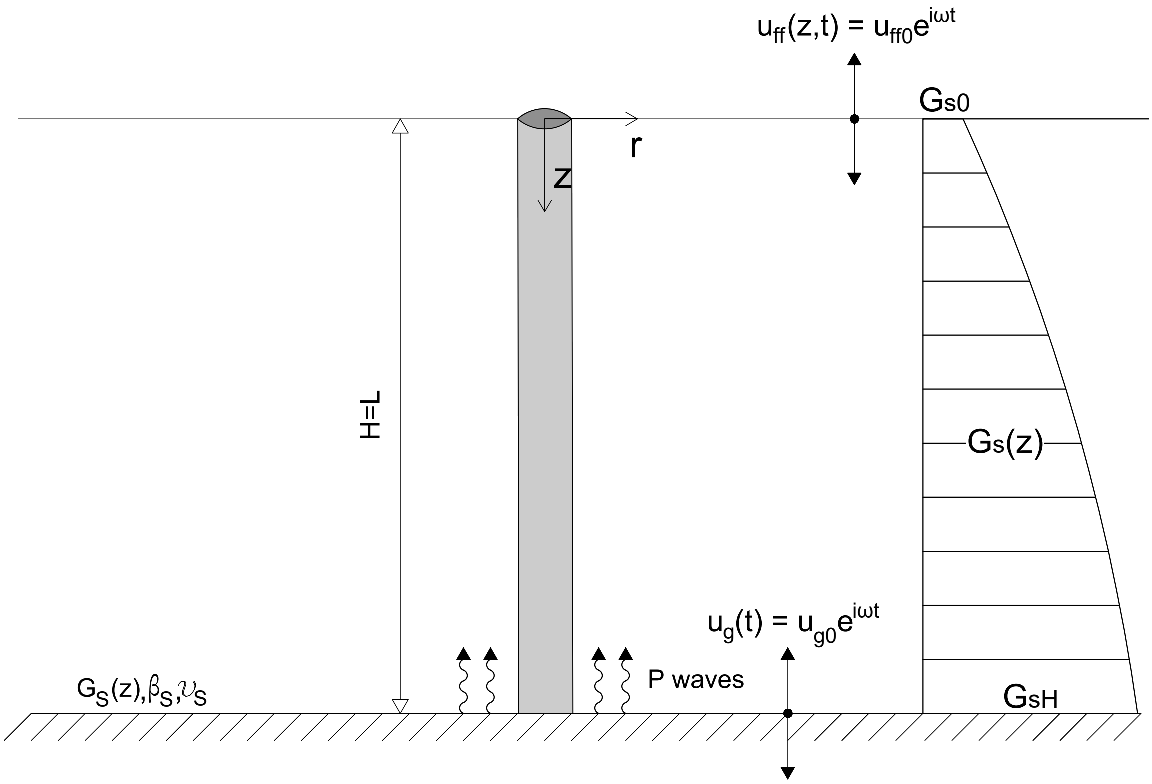

Figure 1: Schematic illustration of a single end-bearing pile resting on a rigid base, embedded in a vertically inhomogeneous soil layer and excited by vertically propagating P-waves.

3 SOIL ANALYSIS

The pile and soil are subjected to vertically harmonic compressional waves (P-waves), expressed through a time-dependent vertical displacement of soil layer base $u_\mathrm{g}(t) = u_\mathrm{g0}\, e^{i\omega t}$, where u_g0 is the displacement amplitude and ω is the cyclic excitation frequency. The equilibrium of the vertical forces acting on a soil element in axisymmetric conditions in cylindrical coordinates yields the governing differential equation [10]

$$\frac{\partial(\tau\, r)}{\partial r} + r\,\frac{\partial\sigma}{\partial z} + r\,\rho_\mathrm{s}\,\frac{\partial^2 u^\mathrm{t}}{\partial t^2} = 0 \tag{2}$$

where $\tau = \tau_{\mathrm{rz}}(r, z, \omega)$ and $\sigma = \sigma_{\mathrm{z}}(r, z, \omega)$ are the vertical soil shear and normal stresses, respectively. u^{t} is the vertical total soil displacement that is expressed as the sum of the rigid base motion u_{g0} and the motion relative to the rigid base u^{r} i.e., $u^{\mathrm{t}} = u^{\mathrm{r}} + u_{\mathrm{g0}}$. The stress-displacement relations for axisymmetric deformations in a Tajimi-type continuum are expressed as follows [18, 20]:

$$\sigma \approx \, - \, \eta_{\mathrm{s}}^2 \, G_{\mathrm{s}}^* \, \frac{\partial u^{\mathrm{r}}}{\partial z} \tag{3}$$

and

$$\tau \approx \, - \, G_{\mathrm{s}}^* \, \frac{\partial u^{\mathrm{r}}}{\partial r} \tag{4}$$

where $\eta_s^2 = 2(1-\nu_{\mathrm{s}})/(1-2\nu_{\mathrm{s}})$ is a compressibility parameter related to the Tajimi approximation. By substituting Equations (3) and (4) into Equation (2), and assuming vertical harmonic soil motion of the form $u = u(r, z, \omega) \, e^{i\omega t}$, the equilibrium equation of stresses can be reformulated in terms of displacements as:

$$\frac{G_{\mathrm{s}}^*}{r} \frac{\partial}{\partial r}\left(r \frac{\partial u^{\mathrm{r}}}{\partial r} \right) \, + \, \eta_s^2 \frac{\partial}{\partial z}\left(G_{\mathrm{s}}^* \frac{\partial u^{\mathrm{r}}}{\partial z} \right) \, + \, \omega^2 \rho_{\mathrm{s}} \left(u^{\mathrm{r}} + u_{\mathrm{g0}} \right) \, = \, 0 \tag{5}$$

The solution to Equation (5) is derived as the sum of the homogeneous solution and a particular solution i.e., $u^{\mathrm{r}} = u_{\mathrm{h}}^{\mathrm{r}} + u_{\mathrm{p}}^{\mathrm{r}}$ (e.g., [10, 6, 22, 24]). The homogeneous solution is found by applying the method of separation of variables, $u = R\,(r) \;\; \Phi\,(z)$, which leads to two ordinary differential equations:

$$R'' + \frac{1}{r} R' - q^2 R \, = \, 0 \tag{6}$$

and

$$\left(\bar{G}_{\mathrm{s}} \Phi' \right)' \, + \, \lambda \, \bar{G}_{\mathrm{s}} \, \Phi \, + \, \left(\frac{\omega}{V_{\mathrm{pH}}^*} \right)^2 \Phi \, = \, 0 \tag{7}$$

Equation (6) represents a linear second-order ordinary differential equation, the solution to which was derived by Mylonakis [25]. Equation (7) is a Sturm–Liouville equation, where Φ denotes the associated eigenfunctions (soil modes). In this equation $\bar{G}_{\mathrm{s}} = G_{\mathrm{s}}^*/G_{\mathrm{sH}}^*$ is a dimensionless soil shear modulus, Φ' is the first derivative of the soil modes Φ with respect to z, and ω/V_{pH}^* represents a complex wave-number which is related to the complex-valued velocity ($V_{\mathrm{p}}^* = V_{\mathrm{p}} \sqrt{1 + 2i\beta_{\mathrm{s}}}$) of vertically propagating P-waves in the soil at $z = H$ (i.e., V_{pH}). q and λ are variables that arise from the application of the method of separation of variables and are linked through the compressibility coefficient as $q = \eta_{\mathrm{s}} \sqrt{\lambda}$. A comprehensive discussion on this topic can be found in the earlier studies of the authors [19, 20]. The particular solution to Equation (5) is expressed in a Fourier series and applying the orthogonality property of the soil modes [10, 6]. The displacements and shear stresses in the soil are expressed in Fourier series as:

$$u^{\mathrm{r}} \, = \, \sum_{m=1}^{\infty} \left[B_m \, K_0(q_m r) \, + \, T_m \, \left(\frac{\omega}{q_m V_{\mathrm{sH}}^*} \right)^2 u_{\mathrm{g0}} \right] \Phi_m \tag{8}$$

and

$$\tau = \sum_{m=1}^{\infty} G_{\mathrm{s}}^{*}\, B_m\, q_m\, K_1(q_m r)\, \Phi_m \tag{9}$$

in which B_m are the corresponding Fourier coefficients, and K_0 and K_1 are the modified Bessel functions of the second kind, zero and first order, respectively. In Equation (8) T_m represents a modal participation coefficient ([10]), which emerged from the expansion of the kinematic excitation in Fourier series i.e., $\left(\omega/V_{\mathrm{sH}}^{*}\right)^2 u_{\mathrm{g0}} \sum_{m=1}^{\infty} T_m\, \bar{G}_{\mathrm{s}}\, \Phi_m$, and can be obtained from:

$$T_m \;=\; \frac{\displaystyle\int_0^H \Phi_m\, dz}{\displaystyle\int_0^H \bar{G}_{\mathrm{s}}\, \Phi_m^2\, dz} \tag{10}$$

4 SOIL-PILE KINEMATIC INTERACTION ANALYSIS

The equilibrium of vertical forces acting on an arbitrary pile segment yields the governing equation of the pile motion:

$$-\,E_{\mathrm{p}}\, A_{\mathrm{p}}\, \frac{\partial^2 \mathrm{w}^{\mathrm{r}}}{\partial z^2} \;+\; \pi\, d\, \tau_0 \;-\; \omega^2 \tilde{m}_{\mathrm{p}} \mathrm{w}^{\mathrm{t}} \;=\; 0 \tag{11}$$

Likewise in soil analysis, the total pile displacement $\mathrm{w}^{\mathrm{t}} = \mathrm{w}^{\mathrm{t}}(z,\omega)$ is expressed as the sum of the motion at the rigid base and the pile displacement relative to the rigid base i.e., $\mathrm{w}^{\mathrm{t}} = \mathrm{w}^{\mathrm{r}} + u_{\mathrm{g0}}$. In the above equation A_{p} is the pile cross-sectional area, $\tilde{m}_{\mathrm{p}}$ is the pile mass density and $\tau_0 = \tau(r = d/2, z, \omega)$ is the vertical shear stress at the soil-pile interface. By substituting Equations (8) and (9) into Equation (11) and integrating along the pile length yields the following equation for evaluating the coupled B_m Fourier coefficients:

$$\begin{aligned} &E_{\mathrm{p}}\, A_{\mathrm{p}} \sum_{m=1}^{\infty} \left(B_m\, K_0(s_m) \;+\; \Lambda^2\, u_{\mathrm{g0}}\, T_m\right) \int_0^H \Phi_m'\, \Phi_k'\, dz + \; 2\,\pi\, s_k\, B_k\, K_1(s_k) \int_0^H G_{\mathrm{s}}^{*}\, \Phi_k^2\, dz \\ &-\; \omega^2\, \tilde{m}_{\mathrm{p}} \sum_{m=1}^{\infty} \left(B_m\, K_0(s_m) + \Lambda^2 u_{\mathrm{g0}} T_m\right) \int_0^H \Phi_m\, \Phi_k\, dz = \; \omega^2\, \tilde{m}_{\mathrm{p}}\, u_{\mathrm{g0}} \int_0^H \Phi_k\, dz \end{aligned} \tag{12}$$

where $\Lambda = \omega/\left(q_m V_{\mathrm{sH}}^{*}\right)$ can be seen as a dimensionless frequency parameter [3]. The pile displacement relative to the rigid base is obtained from Equation (8), considering the perfect bonding at the soil-pile interface:

$$\mathrm{w}^{\mathrm{r}} \;=\; \sum_{m=1}^{\infty} \left(B_m\, K_0(s_m) \;+\; \Lambda^2\, u_{\mathrm{g0}}\, T_m\right)\, \Phi_m \tag{13}$$

where $s_m = q_m\, d/2$ is the dimensionless argument of the Bessel function $K(\,)$.

The stiffer pile diffracts the vertically propagating P-waves in the soil, thereby altering the wave field [1]. To quantify this effect, a kinematic response factor I_{v} is used as the ratio of the total motion at the pile head to the corresponding motion of the free field:

$$I_{\mathrm{v}} \;=\; \frac{\mathrm{w}_0^{\mathrm{t}}}{u_{\mathrm{ff0}}} \tag{14}$$

where the total pile head displacement $\mathrm{w}_0^{\mathrm{t}} = \mathrm{w}_0^{\mathrm{t}}(z = 0, \omega)$ is evaluated from Equation (13) and the total free-field surface motion $u_{\mathrm{ff0}} = u_{\mathrm{ff}}(z = 0, \omega)$ from Equation (8) by letting $r \to \infty$.

5 GENERALISED EIGENVALUE PROBLEM

Equation (7) can be solved by expressing the soil modes $\Phi = \Phi_m(z, \omega)$ in terms of Fourier series as:

$$\Phi_m = \sum_{j=1}^{\infty} S_j^m \, \Psi_j \tag{15}$$

where $S_j^m(\omega)$ are the Fourier coefficients to be determined, and $\Psi_j(z)$ are sinusoidal functions of the form $\cos(\alpha_j z)$, where $\alpha_j = (\pi/2H)(2j-1)$ in which $j = 1, 2, 3, \ldots N$. By substituting Equation (15) into Equation (7), making use of the orthogonality property of the trigonometric functions and integrating along the thickness of the soil layer, yields:

$$\sum_{j=1}^{\infty} S_j^m \int_0^H \bar{G}_{\mathrm{s}} \, \Psi_j' \, \Psi_k' \, dz \; - \; \sum_{j=1}^{\infty} S_j^m \, \lambda_m \int_0^H \bar{G}_{\mathrm{s}} \Psi_j \Psi_k \, dz \; - \; \left(\frac{\omega}{V_{\mathrm{pH}}^*} \right)^2 S_k^m \int_0^H \Psi_k^2 \, dz \; = \; 0 \tag{16}$$

The solution to Equation (16) yields the frequency-dependent eigenvalues λ_m and the corresponding eigenvectors S_j^m.

6 KINEMATIC RESPONSE FACTOR

6.1 Model verification

Figure 2 plots the amplitude of the kinematic response factor, $|I_{\mathrm{v}}|$, with respect to the excitation frequency normalized by the first resonance of the soil deposit (ω/ω_1). The analysis refers to a soil deposit with a linear variation of the shear modulus with depth ($n = 1$ and $b = 0.25$), Eq. (1). Results are presented for two selected soil-pile stiffness contrasts: stiff soils ($E_{\mathrm{p}}/E_{\mathrm{sH}} = 100$) and soft soils ($E_{\mathrm{p}}/E_{\mathrm{sH}} = 1000$), as reported in Figures 2(a) and 2(b), respectively. A soil material damping ratio of $\beta_{\mathrm{s}} = 0.10$ is used. The results are obtained using a Poisson's ratio of $\nu_{\mathrm{s}} = 0.4$ and pile-soil material density ratios determined based on pile-soil stiffness ratios i.e., $\rho_{\mathrm{s}} = \rho_{\mathrm{p}}/1.25$ for $E_{\mathrm{p}}/E_{\mathrm{sH}} < 1000$, and $\rho_{\mathrm{s}} = \rho_{\mathrm{p}}/1.5$ for $E_{\mathrm{p}}/E_{\mathrm{sH}} \geq 1000$. The proposed solution is validated through comparison with finite element (FE) results presented in a recent study by Anoyatis et al. [6] for commonly used piles of pile slenderness ratio $L/d = 25$. Across the full range of excitation frequencies and soil-pile stiffness ratios considered, the proposed model shows excellent agreement with the FE analyses. Specifically, for stiff soils ($E_{\mathrm{p}}/E_{\mathrm{s}} = 100$), the agreement between the proposed solution and FE results is slightly less accurate than for soft soils ($E_{\mathrm{p}}/E_{\mathrm{s}} = 1000$). This discrepancy arises from the limitations of the Tajimi-type continuum in accounting for the increasing influence of radial soil displacement, particularly in stiffer soils. However, this effect is generally minor for typical pile applications in stiff soils.

6.2 Numerical results

The effect of soil inhomogeneity on the kinematic response factor is investigated in Figure 3. In this figure, the kinematic response factors $|I_{\mathrm{v}}|$ are plotted for two selected soil-pile configurations, i.e., $L/d = 10$ (Fig. 3(a)) and $L/d = 25$ (Fig. 3(b)), as functions of the normalized excitation frequency ω/ω_1. The results correspond to a selected distribution of the soil shear modulus with depth: parabolic (dotted line, $n = 0.5$) and linear (dash-dotted line, $n = 1$), Eq. (1). Additionally, results for the special case of a homogeneous soil deposit (solid lines) are included for comparison. All the investigated soil stiffness profiles are characterized by the same soil shear modulus value at depth of $z = H$. The results are presented for both soft soils

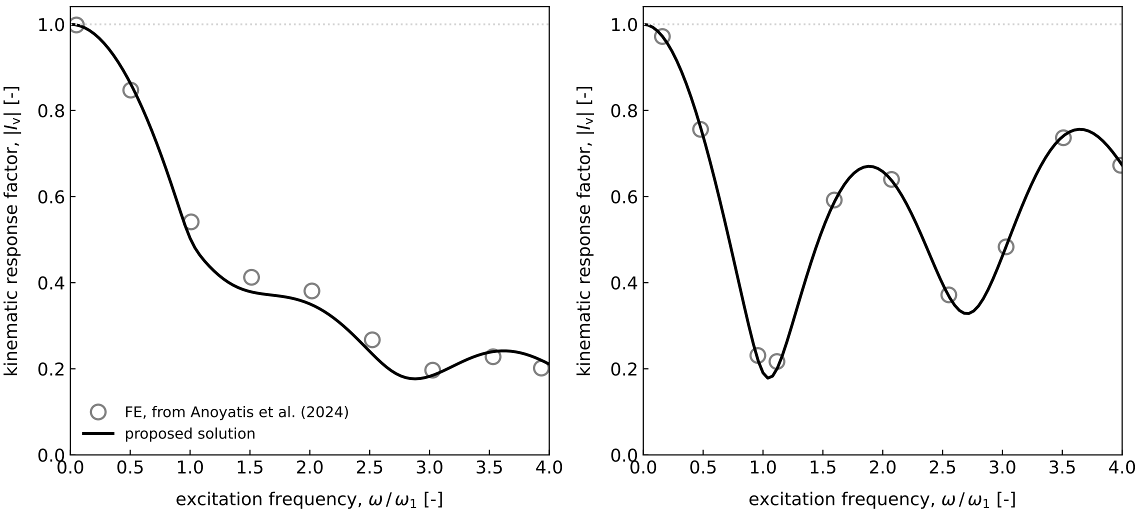

(a) $E_p\,/\,E_{sH} = 100$ (b) $E_p\,/\,E_{sH} = 1000$

Figure 2: Variation of the amplitude of the kinematic response factor $|I_{\mathrm{v}}|$ with normalised excitation frequency ω/ω_1 for a medium with linear variation of the stiffness with depth. Results for: stiff soils with $E_{\mathrm{p}}/E_{\mathrm{sH}} = 100$ (Fig. 2(a)) and soft soils with $E_{\mathrm{p}}/E_{\mathrm{sH}} = 1000$ (Fig. 2(b)). Comparison of the proposed solution with finite element analyses (FE) from Anoyatis et al. [6].

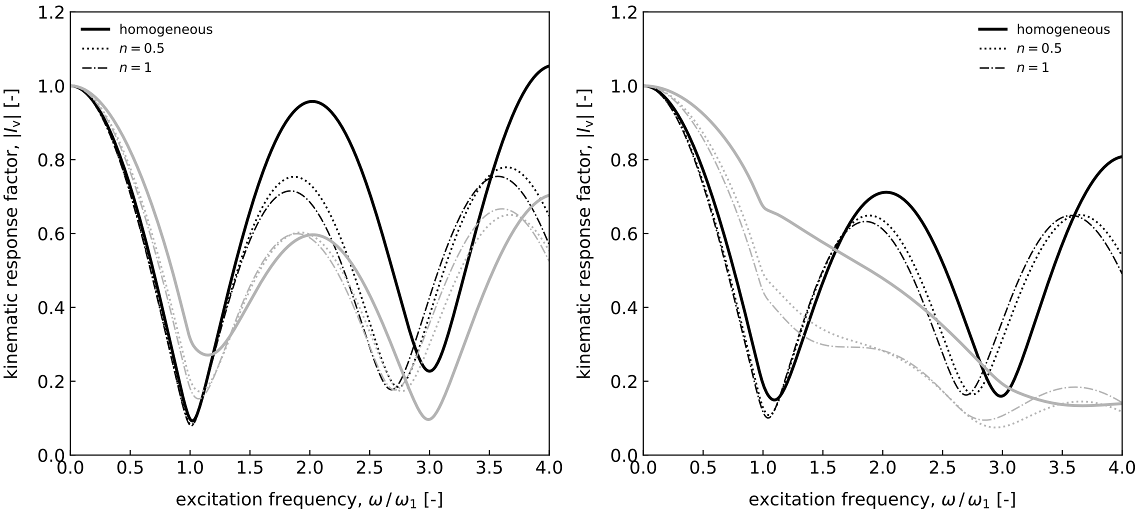

(a) $L/d = 10$ (b) $L/d = 25$

Figure 3: Variation of the amplitude of the kinematic response factor with normalised excitation frequency ω/ω_1 for selected values of the soil inhomogeneity distribution, and for two selected pile slenderness ratios $L/d = 10$ (Fig. 3(a)) and $L/d = 25$ (Fig. 3(b)), for both soft $E_{\mathrm{p}}/E_{\mathrm{sH}} = 1000$ (black curves) and stiff $E_{\mathrm{p}}/E_{\mathrm{sH}} = 100$ (grey curves) soils. $G_{\mathrm{s0}}/G_{\mathrm{sH}} = 0.25$, $\beta_{\mathrm{s}} = 0.05$, $\nu_{\mathrm{s}} = 0.4$, $N = 10$.

($E_{\mathrm{p}}/E_{\mathrm{sH}} = 1000$, in black) and stiff soils ($E_{\mathrm{p}}/E_{\mathrm{sH}} = 100$, in grey). Figures 3 (a) and (b) show that $|I_{\mathrm{v}}| = 1$ at $\omega = 0$, indicating that the pile follows the long-wavelength motion of the soil. Overall, the kinematic interaction factor fluctuates with frequency, attaining values below unity. This suggests that pile foundations typically reduce seismic motion, highlighting their potential filtering effect. An exception occurs in the case of homogeneous soil deposits with $L/d = 10$ (Fig. 3(a)), where $|I_{\mathrm{v}}|$ exceeds unity in the high-frequency range. In general, soil inhomogeneity leads to a reduction in the kinematic response factor $|I_\mathrm{v}|$ over the entire frequency range. The highest $|I_\mathrm{v}|$ is observed in homogeneous soil and decreases as n increases from 0.5 to 1. This trend is attributed to the increased seismic amplification in inhomogeneous soil deposits, which results in larger surface displacements in the free field.

7 CONCLUSIONS

A novel elastodynamic model is derived for the analysis of end-bearing piles embedded in generalised continuously inhomogeneous soils, resting on a rigid rock and excited by vertically propagating P-waves. This study extends the works of Anoyatis et al. [10, 6], enabling the analysis of piles embedded in soil deposits with a generalised variation of the soil stiffness with depth. The response of the pile-soil system is expressed in the form of a generalised Fourier series and the eigenfunctions (soil modes), along the vertical coordinate, are captured by employing simple trigonometric functions. This novel technique avoids solving a laborious eigenvalue problem, thus enhancing computational efficiency. The predictive power of the model is verified through comparisons with finite element analyses across a wide range of excitation frequencies and selected soil-pile stiffness ratios, showing excellent agreement. It is shown that soil inhomogeneity leads to a reduction in the kinematic response factor, $|I_\mathrm{v}|$, across the entire frequency range compared to the homogeneous case, indicating that the filtering effect of piles can be more significant in non-homogeneous soil conditions. Future research will extend the model to accommodate a broader range of applications, including floating piles and pile groups. As a final remark, to ensure results from this research can be verified and reproduced, python scripts and data are shared on a KU Leuven web page titled Soil–Structure Interaction Toolkit, which can be accessed following the link `https://bwk.kuleuven.be/projects/SSItk/` (upon acceptance of the manuscript).

ACKNOWLEDGEMENTS

The research proposed in this paper was supported by KU Leuven through the project "ATHENA Analytical & programming efficiency in geoTecHnical ENgineering Applications" (C24E/22/009), KU Leuven Internal Funds. The authors are grateful for this support.

REFERENCES

[1] G. Gazetas, Seismic response of end-bearing single piles. *International Journal of Soil Dynamics and Earthquake Engineering*, **3**(2), 82–93, 1984. https://www.sciencedirect.com/science/article/pii/0261727784900032.

[2] R. Di Laora, A. Mandolini, and G. Mylonakis, Insight on kinematic bending of flexible piles in layered soil. *Soil Dynamics and Earthquake Engineering*, **43**, 309–322, 2012. https://doi.org/10.1016/j.soildyn.2012.06.020.

[3] G. Anoyatis, R. Di Laora, A. Mandolini, and G. Mylonakis, Kinematic response of single piles for different boundary conditions: Analytical solutions and normalization schemes. *Soil Dynamics and Earthquake Engineering*, **44**, 183–195, 2013. https://doi.org/10.1016/j.soildyn.2012.09.011.

[4] M. Iovino, R. Di Laora, E. Rovithis, and L. de Sanctis, The Beneficial Role of Piles on the Seismic Loading of Structures. *Earthquake Spectra*, **35**(3), 1141–1162, 2019. https://doi.org/10.1193/061318EQS146M.

[5] A. Papazoglou and A. Elnashai, Analytical and field evidence of the damaging effect of vertical earthquake ground motion. *Earthquake Engineering and Structural Dynamics*, **25**(10), 1109–1137, 1996. https://doi.org/10.1002/(SICI)1096-9845(199610)25:10<1109::AID-EQE604>3.0.CO;2-0.

[6] G. Anoyatis, A. Della Corte, O. Orakci, R. Di Laora, A. Tsikas, and S. François, Kinematic response of end-bearing piles in inhomogeneous soils under P-wave excitation. In *Proceedings of the 8th International Conference on Earthquake Geotechnical Engineering*, vol. 10, no. 55, Osaka, Japan, May 7–10, 2024, pp. 2078–2083. https://doi.org/10.3208/jgssp.v10.OS-44-05.

[7] S. M. Mamoon and S. Ahmad, Seismic response of piles to obliquely incident SH, SV, and P waves. *Journal of Geotechnical Engineering*, **116**(2), 186–204, 1990. https://doi.org/10.1061/(ASCE)0733-9410(1990)116:2(186).

[8] F. Ji and R. Y. S. Pak, Scattering of vertically-incident P-waves by an embedded pile. *Soil Dynamics and Earthquake Engineering*, **15**, 211–222, 1996. https://doi.org/10.1016/0267-7261(94)00055-7.

[9] G. Mylonakis and G. Gazetas, Kinematic pile response to vertical P-wave seismic excitation. *Journal of Geotechnical and Geoenvironmental Engineering*, **128**, 860–867, 2002. https://doi.org/10.1061/(ASCE)1090-0241(2002)128:10(860).

[10] G. Anoyatis, R. Di Laora, and G. Mylonakis, Axial kinematic response of end-bearing piles to P waves. *International Journal for Numerical and Analytical Methods in Geomechanics*, **37**(17), 2877–2896, 2013. https://doi.org/10.1002/nag.2166.

[11] D. Dai, M. H. El Naggar, N. Zhang, and Y. Gao, Kinematic response of an end-bearing pile subjected to vertical P-wave considering the three-dimensional wave scattering. *Computers and Geotechnics*, **120**, 103368, 2020. https://doi.org/10.1016/j.compgeo.2019.103368.

[12] D. Dai, M. H. El Naggar, N. Zhang, and Z. Wang, Rigorous solution for kinematic response of floating piles subjected to vertical P-wave. *Applied Mathematical Modelling*, **106**, 114–125, 2022. https://doi.org/10.1016/j.apm.2022.01.031.

[13] D. Dai, K. Xue, Y. Gao, M. H. El Naggar, X. Du, and N. Zhang, Axial kinematic response of an end-bearing pile subjected to seismic P-wave excitation in a double-layered soil. *Soil Dynamics and Earthquake Engineering*, **187**, 109012, 2024. https://doi.org/10.1016/j.soildyn.2024.109012.

[14] C. Zheng, G. Kouretzis, L. Luan, and X. Ding, Kinematic response of pipe piles subjected to vertically propagating seismic P-waves. *Acta Geotechnica*, **16**, 895–909, 2021. https://doi.org/10.1007/s11440-020-01050-3.

[15] C. Zheng, G. Kouretzis, and X. Ding, Seismic response of end-bearing piles in saturated soil to P-waves. *Acta Geotechnica*, **18**(10), 5519–5533, 2023. https://doi.org/10.1007/s11440-023-01942-0.

[16] C. Lin, Q. Liu, T. Deng, et al., Kinematic response of the single floating piles in the two-layered soil subjected to vertically incident P-waves. *Ocean Engineering*, **291**, 116517, 2024. https://doi.org/10.1016/j.oceaneng.2023.116517.

[17] H. Tajimi, Dynamic analysis of structure embedded in an elastic stratum. In *Proceedings of the 4th World Conference on Earthquake Engineering*, vol. 6, 1969, pp. 53–69.

[18] T. Nogami and M. Novak, Soil-pile interaction in vertical vibration. *Earthquake Engineering and Structural Dynamics*, **4**(3), 277–293, 1976. https://doi.org/10.1002/eqe.4290040308.

[19] G. Anoyatis, G. Mylonakis, and A. Tsikas, An analytical continuum model for axially loaded end-bearing piles in inhomogeneous soil. *International Journal for Numerical and Analytical Methods in Geomechanics*, **43**(6), 1162–1183, 2019. https://doi.org/10.1002/nag.2886.

[20] G. Anoyatis, S. François, O. Orakci, and A. Tsikas, Soil–pile interaction in vertical vibration in inhomogeneous soils. *Earthquake Engineering & Structural Dynamics*, **52**(14), 4582–4601, 2023. https://doi.org/10.1002/eqe.3968.

[21] G. Anoyatis, S. François, N. Letizia, A. Della Corte, O. Orakci, and A. Tsikas, Seismic soil pressures on rigid walls retaining inhomogeneous backfills. In *Proceedings of the 18th World Conference on Earthquake Engineering (WCEE 2024)*, Milan, Italy, June 30 - July 5, 2024, technical Session: GEO - Geotechnical Earthquake Engineering and Site Response. https://proceedings-wcee.org/index.html.

[22] A. Della Corte, O. Orakci, A. Tsikas, S. François, and G. Anoyatis, A semi-analytical model for axial soil-pile interaction in generalised inhomogeneous soils. In *Proceedings of the XVIII ECSMGE 2024: Geotechnical Engineering Challenges to Meet Current and Emerging Needs of Society*, Lisbon, Portugal, August 26–30, 2024. https://doi.org/10.1201/9781003431749-58.

[23] A. Della Corte, S. François, A. Tsikas, J. Vankeirsbilck, J. Boydens, and G. Anoyatis, An Analytical Model for Axial Kinematic and Inertial Loading of Piles Embedded in Generalised Inhomogeneous Soils. *Soil Dynamics and Earthquake Engineering*. Available at SSRN: https://ssrn.com/abstract=5074215 or http://dx.doi.org/10.2139/ssrn.5074215 (under revision).

[24] A. Della Corte, N. Letizia, A. Tsikas, S. François, and G. Anoyatis, Dynamic soil pressures on rigid vertical walls in presence of generalised inhomogeneous soils. *Earthquake Engineering and Structural Dynamics*, 2025, (accepted).

[25] G. Mylonakis, Winkler modulus for axially loaded piles. *Géotechnique*, **51**(5), 455–461, 2001. https://doi.org/10.1680/geot.2001.51.5.455.